

The Rarefaction Balancing Method in HSE's PiRRaM Model

Andrew P. L. Newton, Senior Scientist, Health and Safety Executive (HSE), Harpur Hill, Buxton, SK17 9JN, UK
andrew.newton@hse.gov.uk

The Pipeline Release Rate Model (PiRRaM) is used by HSE to predict the transient characteristics of accidental releases from pipelines transporting pressure-liquefied substances (e.g., ammonia, butane, propane and ethylene). PiRRaM is based on DNV PHAST's PipeBreak model (Webber et al., 1999), but includes additional physics, enabling its application to cases where the hole diameter is small in comparison to the pipe diameter. The model smoothly transitions from saturated choked flow for full-bore ruptures and large holes, to incompressible liquid outflow for small holes.

PiRRaM adopts a method for managing the transition between large and small hole behaviour using a rarefaction wave model. Most current models assumed that the contents of the pipe instantaneously decompress to saturated conditions for simplicity. The rarefaction balancing method provides a phenomenological framework to estimate the mass flow rate at the instant the pipe is opened, using the physics of rarefaction waves to bridge the gap between saturated choked flow and incompressible liquid flow.

An additional challenge is linking the initial mass flow rate to the later saturated two-phase flow. PiRRaM addresses this by assuming that the next stage is characterised by a steady-state liquid flow into the orifice, which is choked at the saturated liquid mass flow rate. This implies that the flow in the pipe at the start of the saturated solution may consist of both a stationary zone and an expanding liquid zone. The hole size determines whether only the expanding liquid region is present, or if both the expanding and stationary zones exist. The solution thereafter includes an expanding saturated two-phase flow zone in addition to the expanding and stationary liquid zones.

Full-bore ruptures and large holes correspond to high mass flow rates, where both a stationary and a relatively short expanding liquid zone are likely. In contrast, small holes with much lower mass flow rates have much longer expanding liquid zones, which may exceed the length of the pipe. In this case, the entire pipe is filled with expanding liquid. The key observation is that the amount of mass required to leave the pipe to transition into the saturated flow solution depends on the hole size. This means that for full-bore ruptures, less material is required to be released for the transition to take place than for small holes. Consequently, the transition to saturated flow is predicted to be much more rapid for full-bore ruptures than small holes, which is observed in experiments.

To link the initial mass flow rate to the beginning of the saturated solution, PiRRaM assumes a mass conserving functional form which releases an amount of material depending on the hole size. This is not ideal, as the model in some cases appears to predict unphysical (supersonic) sound wave propagation. However, the error introduced by this approach is acceptably small and the benefits of a consistent approach to link the initial outflow model to the saturated flow solution far outweigh the disadvantages of assuming apparent supersonic sound wave propagation. Model sensitivity and validation evidence for the new model is also presented.

In summary, the rarefaction balancing method is a pragmatic framework which is designed to allow the approach within PipeBreak to be extended to model releases where the hole size is a fraction of the pipe diameter. In such cases the fluid is likely to escape confinement as an incompressible metastable liquid. The approach adds negligible computational burden to the original model, with the entire decompression taking seconds to run. This paper presents important additional details about the model which were not included in the previous Hazards 32 paper describing PiRRaM.

(PiRRaM, HSE, Major Accident Hazard Pipelines, Decompression, Mass Flow Rate, Holes, Liquid Compressibility Effects.)

1 Introduction

The Health and Safety Executive (HSE) uses a computer model, MISHAP (Model for the estimation of Individual and Societal risk from HAZards of Pipelines), to calculate the risks to people, and ultimately the land-use planning (LUP) zones from Major Accident Hazard (MAH) pipelines carrying flammable substances.

MISHAP contains several sub-models to calculate the release rates and the consequences of fireballs and jet fires should a pipeline fail. As part of a programme of continuous development and improvement, the need for a new independent release rate model that would be suitable and adaptable to HSE's future needs and changing IT environments was identified. HSE's PiRRaM (Pipeline Release Rate Model) was developed and has been described in a previous Hazards 32 paper (Newton, 2022). Here, the aim is to provide additional information regarding the development and implementation of PiRRaM, specifically in relation to the transition between the frictionless rarefaction balancing method, and the later saturated two-phase solution.

The issue of modelling the transient decompression of pipelines transporting pressure liquefied fluids has been of interest to loss prevention modellers for some time, and has received considerable attention (Mahgerefteh et al., 2011; Oke et al., 2003; Webber et al., 2010; Yi & Mahgerefteh, 2020). The principal underlying issue is that pressure liquefied fluids escaping confinement can behave as either incompressible liquids, or as choked two-phase releases, depending on the pressurisation above saturation. PiRRaM solves the issue of blending between the different flow regimes using the rarefaction balancing technique.

This paper starts by revising the frictionless rarefaction balancing mechanism and introduces a useful diagram describing the different scenarios that can occur. With the calculation of the initial mass flow rate firmly established, the pressurised liquid

flow solution is derived which allows the characterisation of the conditions at the beginning of the saturated two-phase flow solution. The initial mass flow rate calculation and beginning of the saturated flow represent two important stages in the modelled evolution of the flow. Linking these stages is a mass conserving interpolation method which bridges the gap between the initial frictionless and later frictional flow solutions. The new method is first examined to understand its sensitivity to pipe length, before being compared to experimental data to demonstrate the effectiveness of the rarefaction balancing technique and the assumed interpolation method.

2 High Level Overview

PiRRRaM solves the 1-dimensional quasi-steady compressible pipe-flow equations on the assumption that the fluid in the pipe can be categorised into a maximum of three zones of flow:

- a stationary liquid zone,
- an expanding liquid zone, and
- an expanding two-phase zone.

All three zones may exist simultaneously, though it is possible that only one or two zones may be present depending on the scenario. For example, the pipe is initially assumed to be filled with stationary liquid, whereas later during the decompression the expanding liquid zone or two-phase zone may fill the entire pipe. Combinations are also possible, where the fluid in the pipe is modelled as consisting of an expanding liquid with either an expanding two-phase zone or a stationary zone. If the fluid is a saturated liquid, i.e. it's transported at the saturated vapour pressure and not pressurised above it, then no expanding liquid zone will be present. PiRRRaM uses analytical solutions to the conservation equations to determine the mass of each respective zone for a given mass flow rate before mass conservation is used to build the transient solution from the combination of the mass flow rate and inventory. Newton (2022) provides detailed information describing the model.

The focus of this paper is modelling the transient mass flow rate between the initially stationary liquid state and the point at which two-phase flow begins, which are termed stages 1 and 2 respectively. In stage 1, the rarefaction balancing method is used to estimate the initial mass flow rate. At stage 2, the fluid in the pipe is presumed to consist of an expanding liquid zone¹ with a uniform pressure gradient that is sufficient to provide a mass flow rate corresponding to a choked liquid mass flow rate (Webber et al., 1999). The method is a pragmatic approach to solving the transition between the frictionless rarefaction wave dominated flow and the later friction dominated flow.

Figure 1 shows a schematic plot of the pipe inventory against time during the earliest stage of the release, where the gradient of this line at any point represents the mass flow rate². Stage 1 and Stage 2 are highlighted corresponding to initial mass (M_0 , kg) occurring at moment of opening ($t = 0$, s) and the total mass at the beginning of saturated flow (M_{sat} , kg) which occurs at the later time (t_{sat} , s). The mass flow rates at Stages 1 and 2 are given by the rarefaction balancing method (\dot{m}_0 , kg s⁻¹), kg s⁻¹) and the choked saturated liquid outflow model (\dot{m}_{sat} , kg s⁻¹) respectively. In essence, the following calculations therefore relate to calculating: 1) the initial mass flow rate (\dot{m}_0); 2) the total mass at the beginning of saturated flow (M_{sat}); 3) the time when saturated two-phase flow starts (t_{sat}); and 4) a mass conserving interpolation method. The following sections therefore describe the rarefaction balancing method, the pressurised liquid flow solution, and the interpolation method.

¹ A stationary liquid zone may be present depending on the length of pipe and the hole size.

² In Figure 1, \dot{m} is represented as the derivative of the pipe inventory and is consequently a negative value,

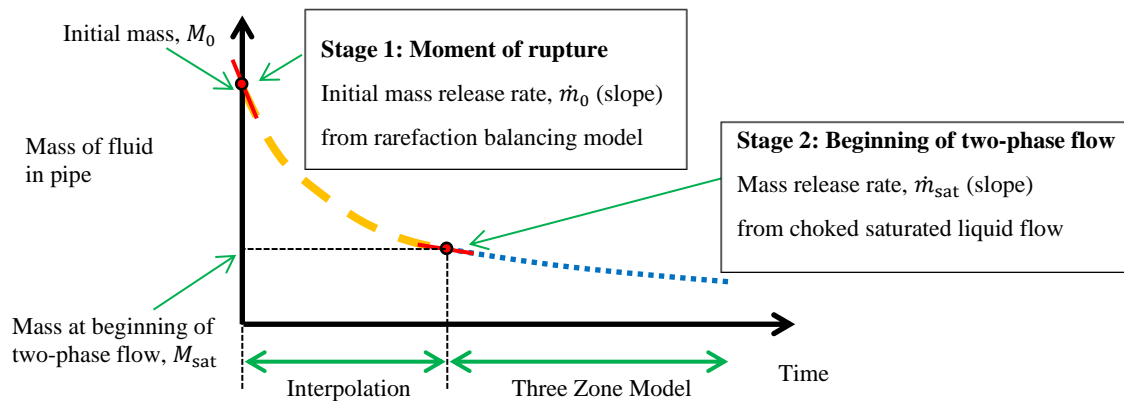


Figure 1: Schematic showing the interpolation used during the initial decompression from pressurised conditions.

3 The Rarefaction Balancing Mechanism

3.1 Background

This section focuses on the initial mass flow rate of liquid released from the pipeline immediately after the pipeline is punctured or ruptured. The basis for this analysis is the phenomenological mass balancing equation, which itself emerges from a generalisation of a similar calculation for ideal gas cases given in Landau and Lifshitz (1987). The mass balancing equation is given by:

$$A_{\text{hole}}G_{\text{hole}}(P_d) = A_{\text{pipe}}G_{\text{rarefaction}}(P_d) \quad (1)$$

Where:

- A_{hole} is the area of the hole (m^2)
- A_{pipe} is the internal cross-section area of the pipe (m^2)
- $G_{\text{hole}}(P_d)$ is the mass flux density of fluid leaving through the hole ($\text{kg m}^{-2}\text{s}^{-1}$)
- $G_{\text{rarefaction}}(P_d)$ is the mass flux density of fluid in the pipe due to the rarefaction expansion ($\text{kg m}^{-2}\text{s}^{-1}$)
- P_d is the pressure downstream of the rarefaction wave (Pa)

This equation describes how the rarefaction wave provides a mass flow rate into a frictionless zone that, for reasons of mass conservation, needs to balance the mass release rate out of the pipe. The following process is therefore referred to as the rarefaction balancing outflow model. The following assumptions are made in the initial flow rate model:

Rarefaction Balanced Outflow Assumption 1: Discharge Coefficient

For the bounding case in the new model, where the unchoked flow model is used (i.e. Bernoulli's equation for incompressible flow), it is assumed the discharge coefficient is $c_d = 1$ for a full-bore rupture (FBR), and $c_d = 0.6$ for all other holes smaller than full-bore rupture. For the other bounding case involving choked flow, the discharge coefficient is assumed implicitly to be $c_d = 1$.

Rarefaction Balanced Outflow Assumption 2: Bernoulli and Saturated Two-phase Flow Models

Two bounding cases are used to model choked and unchoked flow, i.e. the saturated two-phase pipeline model and Bernoulli's equation, these have their own implicit assumptions.

Bernoulli's equation for incompressible flow with $c_d \approx 0.6$ has been found to accurately predict the release rates from vessels containing flashing liquids through circular holes, at pressures equalling or exceeding their saturation vapour pressure (Britter et al., 2011; Richardson et al., 2006). Steady state releases of compressed liquid through pipes with holes at the end recover the same behaviour when the hole is sufficiently small (Cowley and Tam, 1988). As such, unchoked liquid outflow is assumed to be the upper limit on the likely mass flow rate for compressed flows.

3.2 Regime Diagram

Figure 2 shows regime diagram which plots the conditions corresponding to between different outflow regimes, and the transitions between them. The outflow regimes are governed by the dimensionless pressure (the initial pressure normalised

by the initial saturated vapour pressure, ($P_0^* = P_0 P_{\text{sat}}(T_0)^{-1}$) as a function of the dimensionless rupture/hole area (hole area normalised by the pipe area³, $A_{\text{hole}}^* = A_{\text{hole}} A_{\text{pipe}}^{-1}$). There are four zones in the regimes diagram: a zone of unchoked liquid flow for sufficiently large pressures (brown shading); a zone where choked saturated flow is likely (light blue); a transition zone where the flow is limited by the rarefaction wave (light green zone); and a zone corresponding to saturated two-phase initial conditions which is outside the scope of the current investigation as two-phase initial conditions are not considered by HSE.

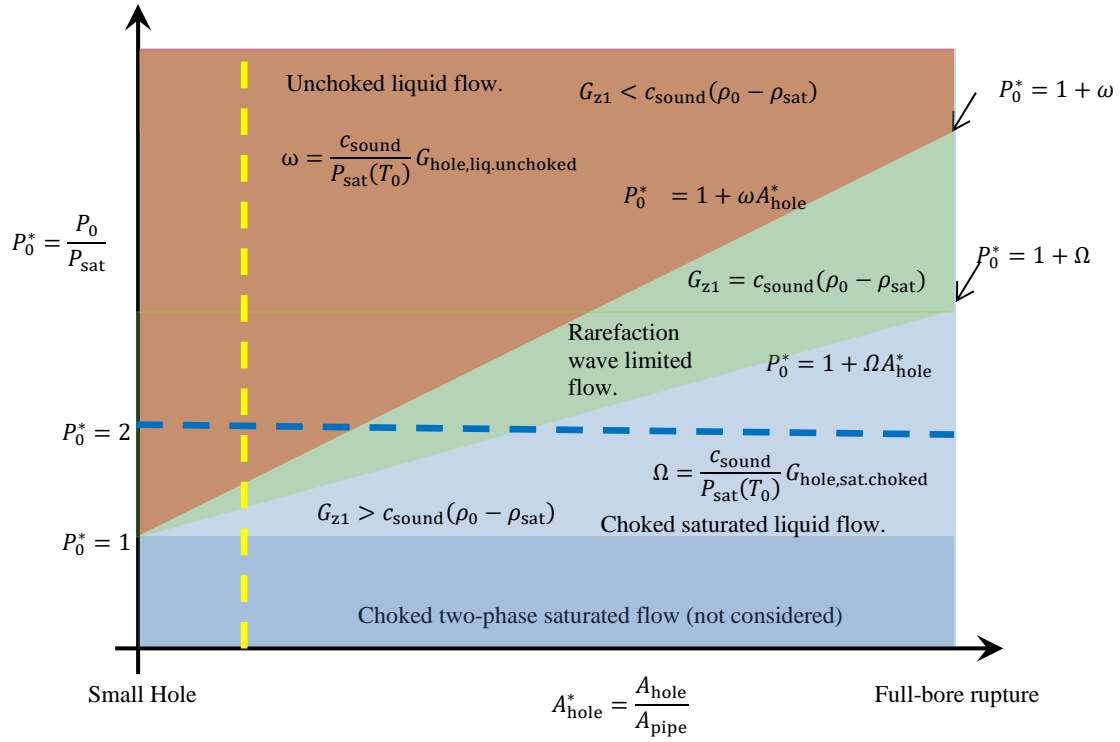


Figure 2 Regime diagram plotting the dimensionless pressure (P_0^*) against the dimensionless hole area (A_{hole}^*). The brown shaded area indicates unchoked liquid outflow, green shaded region indicates rarefaction wave limited outflow, and light blue shaded zone indicates saturated choked flow. This diagram is only indicative: the slopes of the two lines, ω and Ω are dependent upon material properties and the initial temperature. The region $P_0^* < 1$ (dark blue shaded area) is out of scope as this corresponds to a two-phase flow initial condition.

In the unchoked liquid outflow zone (brown), the mass flow rate contribution from the rarefaction wave is sufficient to drive an incompressible liquid outflow at a mass flow rate significantly exceeding the saturated choked flow value. In the choked saturated liquid flow zone (light blue), the rarefaction wave is weak, and it is assumed that the outflow corresponds to a saturated choked flow. The transitional flow regime (green zone) is referred to as the rarefaction balanced outflow. Here, the rarefaction wave produces a mass flow rate exceeding the choked flow value, but insufficient to balance liquid outflow, and the mass flow rate is chosen to be the rarefaction balanced mass flow rate. The lines formally defining the transition between these regimes are introduced in the subsequent sections.

Also shown in Figure 2 are lines indicating constant hole area and variable pressure (the vertical dashed yellow line), and fixed initial pressure and varying hole area (dark blue dashed line). These are used in later sections to qualitatively discuss the behaviour of the model.

³ For the case of a hole midway along a pipe, either the pipe area needs to be doubled or the hole area halved, to account for the pipes on both side of the hole contributing to the release and doubling the area of the rarefaction wave.

3.3 Rarefaction Balancing and the Regime Diagram

The following analysis derives the switching criteria based upon the consideration of the pressure difference between two positions: the first is in the undisturbed fluid at the upstream edge of the rarefaction wave; and the second is at the discharge plane. It is important here to be clear about the use of notation to identify which parameters are involved.

The conditions upstream of the rarefaction wave are denoted by a subscript 0, and the conditions downstream of the rarefaction wave are denoted with a subscript d. Assuming that the liquid is initially stationary⁴, i.e. ($U_0 = 0$), the rarefaction mass flux density (mass flow rate per unit area associated with a drop in pressure from P_0 to P_d , denoted by $G_{\text{rarefaction}}$) is given by:

$$G_{\text{rarefaction}} = c_{\text{sound}}(\rho_0 - \rho_d) \quad (2)$$

where ρ_d (kg m^{-3}) is the density in the frictionless zone downstream of the rarefaction wave where the pressure is P_d (Pa), and c_{sound} (m s^{-1}) is the liquid sound speed. As the pressure is uniform in this zone, P_d is also occasionally referred to as the orifice pressure. It is assumed that this loss of liquid from the pipeline from the rarefaction wave is balanced by either a choked or an unchoked liquid outflow at the orifice. These two scenarios are described in the next two subsections.

3.3.1 Rarefaction Balanced by Choked Liquid Outflow

This section determines the conditions at which the mass flow rate corresponding to the rarefaction wave and choked saturated liquid outflow match exactly.

In the scenario where the rarefaction is balanced by choked liquid outflow, the pressure at the discharge plane, P_d , is equal to the saturation vapour pressure, P_{sat} . The mass flux density ($G_{\text{hole,sat,choked}}$, $\text{kg m}^{-2}\text{s}^{-1}$) through the orifice is calculated from the equation given in Webber et al. (1999), which is reproduced below for an incompressible liquid:

$$G_{\text{hole,sat,choked}} = \frac{\phi}{\sqrt{T_0 c_p - \phi \rho_{\text{sat}}^{-1}}} \quad (3)$$

Here, ϕ is given by Clausius Clapeyron relationship $\phi = T_0 \frac{dP_{\text{sat}}}{dT} \Big|_{T=T_0}$ (Pa), where $\frac{dP_{\text{sat}}}{dT}$ (Pa K^{-1}) is the gradient of the saturated vapour pressure with respect to temperature, and ρ_{sat} (kg m^{-3}) is the saturated liquid density, and c_p is the specific heat at constant pressure (J/kg/K). To determine when these conditions apply, the starting point is the equation for the mass flux density driven by rarefaction, where the density at the discharge plane, ρ_d , is taken to be the liquid density at the saturation vapour pressure, ρ_{sat} . The equation for $G_{\text{rarefaction,max}}$ is then given by:

$$G_{\text{rarefaction,max}} = c_{\text{sound}}(\rho_0 - \rho_{\text{sat}}) \quad (4)$$

To conserve mass, the mass flux from the liquid rarefaction along the whole pipe cross-section ($A_{\text{pipe}}G_{\text{rarefaction}}$) must balance the choked mass flux of saturated liquid through the hole in the pipeline ($A_{\text{h}}G_{\text{hole,sat,choked}}$) via:

$$A_{\text{pipe}}G_{\text{rarefaction,max}} = A_{\text{hole}}G_{\text{hole,sat,choked}} \quad (5)$$

and therefore:

$$c_{\text{sound}}(\rho_0 - \rho_{\text{sat}}) = \frac{A_{\text{hole}}}{A_{\text{pipe}}}G_{\text{hole,sat,choked}} \quad (6)$$

which can also be written using the definition of the speed of sound⁵ as:

$$\frac{(P_0 - P_{\text{sat}})}{c_{\text{sound}}} = \frac{A_{\text{hole}}}{A_{\text{pipe}}}G_{\text{hole,sat,choked}} \quad (7)$$

Here P_{sat} is the saturation vapour pressure at the initial temperature, T_0 . Rearranging the above equation to express it in terms of the ratio of the initial pressure to the saturation vapour pressure gives:

⁴ The effect of pumping is likely to be insignificant as the fluid speed is low in comparison to the sound speed and will likely cancel out in the case of a release from the pipe midpoint.

⁵ The speed of sound (c_{sound} , m s^{-1}) in a fluid is given by $c_{\text{sound}}^2 = \frac{dP}{d\rho} \Big|_{\Delta S=0}$ where the derivative of pressure with respect to density is evaluated at constant entropy.

$$\frac{P_0}{P_{sat}} = 1 + \frac{c_{sound} A_{hole}}{P_{sat} A_{pipe}} G_{hole,sat,choked}. \quad (8)$$

To aid interpretation of the underlying physics, (8) is expressed in terms of the pressure ratio ($P_0^* = P_0/P_{sat}$) and area ratio ($A_{hole}^* = A_{hole}/A_{pipe}$).

$$P_0^* = 1 + \Omega A_{hole}^*, \text{ where } \Omega = \frac{c_{sound}}{P_{sat}} G_{hole,sat,choked}. \quad (9)$$

The quantities A_{hole}^* and P_0^* represent the horizontal and vertical axis of the regime diagram in Figure 2.

3.3.2 Rarefaction Balanced by Unchoked Liquid Outflow

This section finds the conditions at which the mass flow rates corresponding to the rarefaction wave and unchoked liquid outflow match exactly.

In the scenario where the rarefaction is perfectly balanced by unchoked liquid outflow, the mass flux density ($G_{hole,liq,unchoked}$, $\text{kg m}^{-2}\text{s}^{-1}$) is calculated from Bernoulli's equation for incompressible liquid flow as follows:

$$G_{hole,liq,unchoked} = c_d \sqrt{2\rho_d(P_d - P_{atm})} \quad (10)$$

where the coefficient of discharge is either⁶ $c_d = 1$ for full-bore ruptures, or $c_d = 0.6$ for any holes with an area smaller than the full cross-sectional area of the pipe.

The pressure, P_d , in the above equation is found by balancing the unchoked liquid outflow against the mass release rate driven by rarefaction, i.e.

$$A_{pipe} G_{rarefaction} = A_{hole} G_{hole,liq,unchoked} \quad (11)$$

which upon substitution of (2) and (10) becomes:

$$A_{pipe} c_{sound} (\rho_0 - \rho_d) = A_{hole} c_d \sqrt{2(P_d - P_{atm})\rho_d} \quad (12)$$

where the density (ρ_d , kg m^{-3}) is evaluated at the initial temperature, (T_0 , K) and the pressure (P_d , Pa) using the Reid et al. (1987) equation of state (specifically the Thomson extension of the Hankinson-Brobst-Thomson (HBT) method for compressed liquids, although any accurate EOS can be used). The speed of sound (c_{sound} , m s^{-1}), is estimated from:

$$c_{sound} = \sqrt{\frac{P_0 - P_d}{\rho_0 - \rho_d}} \quad (13)$$

and (12) is solved numerically to find the pressure, P_d . Once this pressure is known, it can be used to find the mass flux density through the hole using Bernoulli's equation for incompressible flow, (see ((10))).

To find the set of conditions under which the rarefaction is balanced by unchoked liquid outflow, the limiting case is considered where the pressure at the discharge plane is the saturation vapour pressure, $P_d = P_{sat}(T_0)$. Balancing the mass flow rates for this scenario then provides:

$$\frac{(P_0 - P_{sat})}{c_{sound}} = \frac{A_{hole}}{A_{pipe}} G_{hole,liq,unchoked} \quad (14)$$

which can be rearranged in terms of the pressure ratio (P_0/P_{sat}) as follows:

$$\frac{P_0}{P_{sat}} = 1 + \frac{c_{sound} A_{hole}}{P_{sat} A_{pipe}} G_{hole,liq,unchoked} \quad (15)$$

As before, the above equation can be expressed in terms of the pressure ratio ($P_0^* = P_0/P_{sat}$) and area ratio ($A_{hole}^* = A_{hole}/A_{pipe}$), which represent the vertical and horizontal axis of the regime diagram in Figure 2:

⁶ HSE's method for modelling releases from pipelines assumes prescribed hole sizes, and it is not necessary to include a smooth transition for the coefficient of discharge between the full-bore rupture and hole scenario, as the hole will always be sufficiently small to justify using $c_d = 0.6$.

$$P_0^* = 1 + A_{\text{hole}}^* \frac{c_{\text{sound}}}{P_{\text{sat}}} G_{\text{hole,liq,unchoked}} = 1 + \omega A_{\text{hole}}^* \quad (16)$$

where the slope of the line in the regime diagram that delineates unchoked flow is the parameter ω , which is given by:

$$\omega = \frac{c_{\text{sound}}}{P_{\text{sat}}} G_{\text{hole,liq,unchoked}} = \frac{c_{\text{sound}}}{P_{\text{sat}}} c_d \sqrt{2(P_{\text{sat}} - P_{\text{atm}}) \rho_d} \quad (17)$$

In the above equation, the saturation vapour pressure and the liquid density are evaluated at the initial temperature (T_0).

3.3.3 Further discussion of the Regime Diagram

The regime diagram shown in Figure 2 provides an intuitive understanding of the decompression process. It is now possible to formally define the transitions between the different zones. Specifically, (9) corresponds to the transition between saturated choked outflow and rarefaction wave limited flow, and (16) corresponds to the transition between rarefaction wave limited flow and pressure liquefied flow. A more thorough interpretation of these zones is now possible, which is presented below.

Unchoked flow

The top left (coloured brown) in Figure 2 corresponds to case where the initial pressure is sufficiently high to guarantee an incompressible liquid outflow. This is defined by the condition:

$$P_0^* \geq 1 + \omega A_{\text{hole}}^* \quad (18)$$

Within this region, the initial mass flow rate is calculated using Bernoulli's equation for unchoked liquid flow, i.e.

$$\dot{m}_0 = c_d A_{\text{hole}} \sqrt{2(P_d - P_{\text{atm}}) \rho_d} \quad (19)$$

Where the pressure downstream of the rarefaction wave (P_d) is calculated by numerically solving (12). The physical interpretation of this region is the situation where the initial expansion of the liquid as the rarefaction wave passes up the pipeline provides more than enough liquid to maintain an unchoked release.

Choked flow

The lower right region (coloured in light blue) in Figure 2 is where the initial pressure is close to the saturation vapour pressure and/or the hole is large. This is defined by the equation:

$$1 < P_0^* \leq 1 + \Omega A_{\text{hole}}^* \quad (20)$$

Within this region, the initial mass flow rate is calculated using the equation for choked flow at the saturation vapour pressure (3).

The initial expansion of the liquid as the rarefaction wave passes up the pipeline does not provide sufficient liquid to maintain unchoked flow through the large orifice, the pressure falls practically instantaneously to the saturation vapour pressure, and the discharge rate is then governed by the choked flow rate for a saturated liquid.

Rarefaction Wave Limited Outflow - Transitional Flow

Between the two regions defined above is a third region (coloured in green in the regime diagram), defined by the criteria:

$$1 + \Omega A_{\text{hole}}^* < P_0^* < 1 + \omega A_{\text{hole}}^* \quad (21)$$

Within this transitional region, for a given pressure, the mass flow rate is assumed to remain constant as the hole size varies between the upper and lower bounding cases of choked and unchoked flow. The initial mass flow rate is given by the rarefaction mass flow rate:

$$\dot{m}_0 = A_{\text{pipe}} c_{\text{sound}} (\rho_0 - \rho_{\text{sat}}) \quad (22)$$

where the saturated liquid density, ρ_{sat} , is evaluated at the initial temperature, T_0 .

Figure 3 and Figure 4 qualitatively show the mass flow rate and mass flux density behaviour corresponding to a hypothetical substance for cases on the blue and yellow dashed lines in Figure 2. In both plots, the mass flow rate is plotted in purple using the left ordinate axis, and the mass fluid density is plotted in red using the right ordinate axis.

Figure 3 show the variation of the mass flow rate and mass flux density for varying the hole area, for cases where initial pressure that is nominally twice the saturated vapour pressure (see the horizontal dashed blue line in Figure 2). As the hole

size decreases from a full-bore rupture, Figure 3 shows how the outflow is initially saturated and choked with a uniform mass flux density, corresponding to a linearly decreasing mass flow rate, down to the beginning of the transition zone at $A_{hole}^* = \Omega^{-1}$. In the transition zone, $\omega^{-1} < A_{hole}^* < \Omega^{-1}$, the mass flow rate is constant, but the mass flux density (red line) increases to the unchoked liquid outflow value at $A_{hole}^* = \omega^{-1}$. For $A_{hole}^* < \omega^{-1}$, the mass flow rate continues to decrease as the mass flux density increases to the value corresponding to an equivalent release from a vessel at the initial pipeline pressure. The important point to note is that there is no step change in the initial mass flow rate.

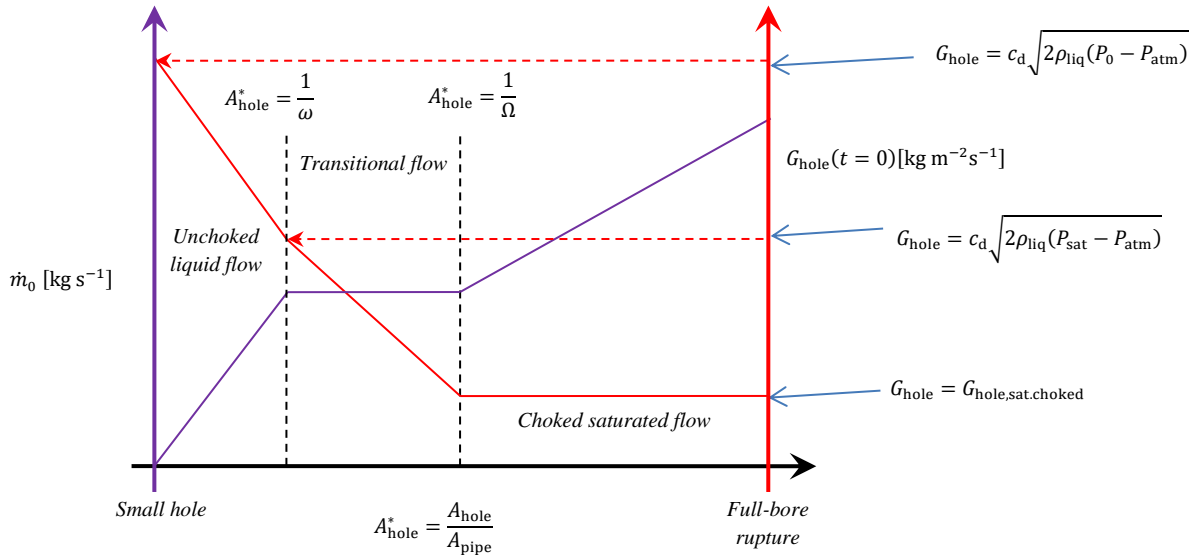


Figure 3 Illustration of the mass flow rate \dot{m}_0 (purple line/left ordinate axis) and mass flux density G_{hole} (red line/right ordinate axis) versus the dimensionless hole-area (A_{hole}^*), for $P_0^* = 2$ (i.e. representing the mass flow rate/mass flux density behaviour along the horizontal blue dashed line in Figure 2).

To further illustrate the behaviour shown in the regime diagram, Figure 4 shows the change in mass flow rate and mass flux density as the pressure is increased whilst the hole size is held constant (a hole that is 1/10th of the pipe cross sectional area - the vertical dashed yellow line shown in Figure 2). In this case, as the pressure increases from saturation, there is initially no change in the mass flow rate until the beginning of the transition zone, after which the mass flow rate increases monotonically with pressure, which continues through both the transition zone and the unchoked liquid flow zone.

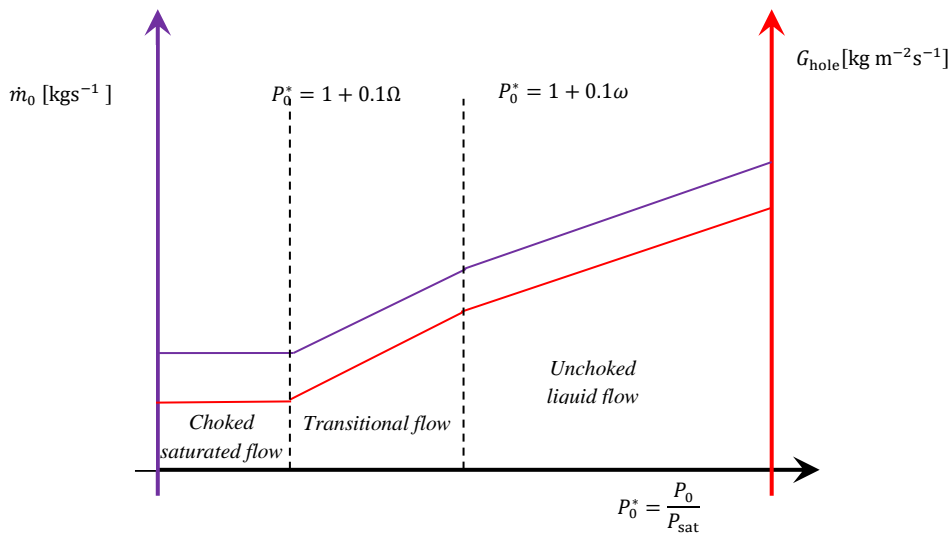


Figure 4: Schematic diagram qualitatively indicating mass flow rate \dot{m}_0 (purple line/left ordinate axis) and mass flux density G_h (red line/right ordinate axis) versus the dimensionless pressure P_0^* , for $A_{hole}^* = 0.1$ (i.e. the vertical yellow line at $A_{hole}^* = 0.1$ in Figure 2).

4 The Pressurised Liquid Flow Solution.

4.1 Introduction

This section describes the theoretical foundations of the expanding liquid flow model (zone 1) in more detail. In the following, the terminology “compressed” or “pressurised” refer to a fluid that is stored at a pressure that exceeds its saturation vapour pressure, and stored at a temperature exceeding its boiling temperature at atmospheric pressure. The objective of this section is to derive the equations describing the length and mass of the single phase, expanding pressurised liquid zone.

Assumptions

1. Isothermal decompression
2. Approximate linear equation of state for compressed liquid
3. Uniform pressure gradient in expanding zone
4. Isobaric process linking conditions immediately upstream of the orifice to conditions on the orifice plane.

Isothermal Decompression

The first assumption is that the decompression of the fluid from its initial pressurised state to the saturation vapour pressure is isothermal, i.e. the temperature remains constant at the initial value, T_0 , as the pressure changes from its initial value, P_0 , to the saturation pressure P_{sat} .

This assumption of isothermal decompression is also adopted in the PipeBreak model in PHAST, DNV (2011). A real fluid will likely decompress with constant entropy and lead to some cooling. The magnitude of the temperature change is uncertain. Previous validation of the PipeBreak model, with this assumption of isothermal decompression, against the Isle of Grain data (Richardson & Saville, 1996) showed that temperature after the decompression to saturation was relatively unchanged.

Assuming isothermal decompression makes the derivation of the new model considerably easier. The effect of isothermal decompression is likely to be most significant near critical conditions. However, the decompression is usually associated with a temperature drop, which causes a lower choked mass flux density. It is therefore arguable that assuming isothermal decompression is conservative.

Approximate Equation of State

The second assumption relates to assuming a simplified equation of state for the compressible liquid. Since it is assumed that decompression of the liquid is isothermal, the liquid density is required as a function of pressure. The density of a liquid generally changes only slightly over a large pressure range. The third assumption in deriving the new model is that the density varies linearly with pressure. Figure 5 plots the density against pressure for propane at 5°C between the saturated vapour pressure and 100 bar using Reid et al. (1987) (specifically the Thomson extension of the Hankinson-Brobst-Thomson (HBT) method⁷ for compressed liquids), and demonstrates that the interpolation between endpoints is an acceptable approximation.

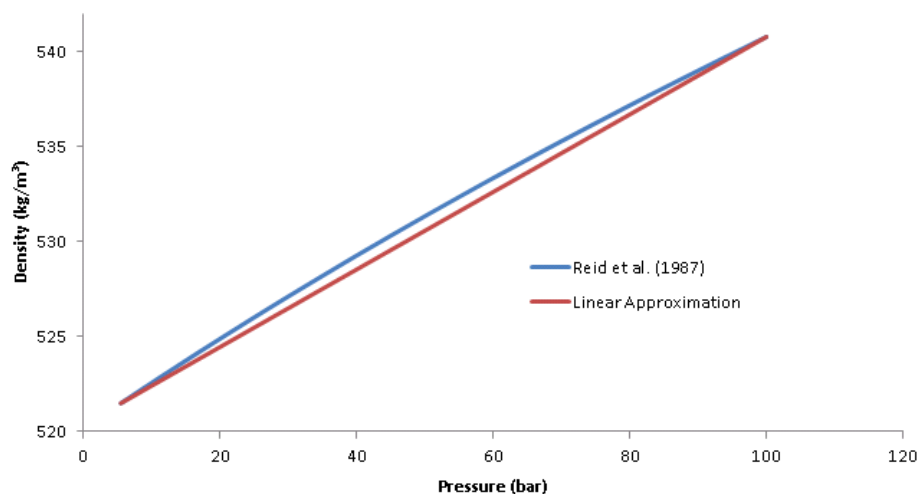


Figure 5 Density of propane at 5°C calculated using the Hankinson-Brobst-Thomson method and the linear approximation.

The liquid density is therefore approximated as a function of pressure via:

$$\rho = \rho_{sat} + \frac{\rho_0 - \rho_{sat}}{P_0 - P_{sat}}(P - P_{sat}). \quad (23)$$

where the densities, ρ_0 and ρ_{sat} , are calculated using an appropriate equation of state.

⁷ The HBT method is valid for temperatures up to 95% of the value of the critical temperature ($T/T_{crit} < 0.95$). For cases that are closer to the critical point, PiRRaM fixes T at $0.95T_{crit}$ (Reid et al., 1987).

Uniform Pressure Gradient

In the zone of pressurised liquid flow, the pressure is a linear function of distance along the pipe (uniform pressure gradient). This is a direct consequence of the fluid being weakly compressible, and the mass flux density being uniform in moving sections of the pipe. The consequence is that the density varies linearly between the upstream and downstream ends of the compressed liquid zone within the pipeline. This allows the mass in the compressed pure liquid zone of the pipe to be calculated.

Exit Pressure and Holes

This model applies to a specific case corresponding to saturated choked flow through the orifice. As such, the exit pressure is always saturated, and the pipe mass flux density is found by assuming a mass conserving, isobaric and isothermal process linking the flow at the pipe cross sectional area to the flow on the orifice plane.

4.2 Derivation

4.2.1 Length of Expanding Liquid Zone

Assuming quasi-steady flow (i.e. omitting time derivatives and also convective acceleration), the momentum conservation equation becomes (Webber et al., 1999):

$$\frac{dP}{dx} = -2f \frac{G_{z1}|G_{z1}|}{D\rho_{sat}} \quad (24)$$

where:

- P is the pressure (Pa)
- x is the axial distance along the pipe (m)
- $f = \left(4\log_{10} \frac{3.7D}{\epsilon}\right)^{-2}$ is the Fanning friction calculated using the Haaland (1983) correlation (-)
- ϵ is the pipe surface roughness⁸ (m)
- ρ_{sat} is the saturated liquid density⁹ (kg m⁻³)
- D is the diameter of the pipe (m)
- $G_{z1} = \frac{A_{hole}}{A_{pipe}} G_{hole}$ is the mass flux density in the expanding liquid zone (kg m⁻²s⁻¹)s⁻¹

The mass flux density, G_{hole} , is calculated using the rarefaction balancing method. Integrating (24) over the expanding liquid region for a right to left flow gives the following equation for the length of the expanding liquid (L_{z1}) zone:

$$L_{z1} = \frac{D\rho_{sat}(P_0 - P_{sat})}{2fG_{z1}^2} \quad (25)$$

4.2.2 Mass of Pressurised Liquid in Zone 1

The mass of pressurised liquid in zone 1, M_{z1} , per unit cross-sectional area of the pipeline, A_{pipe} , is calculated by integrating the density along the pipe:

$$\frac{M_{z1}}{A_{pipe}} = \int_{x_{sat}}^{x_0} \rho dx \quad (26)$$

between positions $x_{sat} = 0$ and $x_0 = L_{z1}$, where x (m) is the axial distance along the pipe from the orifice. The pressure gradient is assumed to be uniform in the expanding liquid zone (liquid flow assumption 3), the consequence of which is that the density varies linearly along the pipe i.e.

$$\rho = \rho_{sat} + \frac{\rho_0 - \rho_{sat}}{P_0 - P_{sat}} (P - P_{sat}) \quad (27)$$

⁸ Surface roughness is typically taken to be $\epsilon = 4.5 \times 10^{-5}$ m.

⁹ The expanding zone length calculation is not sensitive to slight variations in the liquid density, and the saturated liquid density is chosen arbitrarily.

where $(x_0 - x_{sat}) = L_{z1}$ in the above expression is the length of zone 1. The equation for the mass per unit area then becomes:

$$\frac{M_{z1}}{A_{\text{pipe}}} = \int_0^{L_{z1}} \rho_{\text{sat}} + x \frac{(\rho_0 - \rho_{\text{sat}})}{L_{z1}} dx \quad (28)$$

which integrates to:

$$\frac{M_{z1}}{A_{\text{pipe}}} = \left[\rho_{\text{sat}}x + \frac{x^2 (\rho_0 - \rho_{\text{sat}})}{2 L_{z1}} \right]_0^{L_{z1}} \quad (29)$$

which evaluates to:

$$\frac{M_{z1}}{A_{\text{pipe}}} = L_{z1} \frac{\rho_0 + \rho_{\text{sat}}}{2} \quad (30)$$

The mass required to be lost in zone 1 to reach saturated conditions ($\Delta M_{L_{\text{pipe}} > L_{z1}}$) is therefore:

$$\Delta M_{L_{\text{pipe}} > L_{z1}} = M_0 - M_{\text{sat}} = A_{\text{pipe}} L_{z1} \left(\rho_0 - \frac{\rho_0 + \rho_{\text{sat}}}{2} \right) = A_{\text{pipe}} L_{z1} \left(\frac{\rho_0 - \rho_{\text{sat}}}{2} \right) \quad (31)$$

4.2.3 Upstream Conditions

When calculating L_{z1} it is possible that the length of pipe required to drop the pressure from P_0 to $P_{\text{sat}}(T_0)$ for the given G_{z1} , might exceed the available length of pipe ($L_{\text{pipe}} < L_{z1}$). In this scenario, the upstream pressure will fall beneath the initial value. To accurately calculate the inventory mass, the upstream pressure needs to be calculated.

If zone 1 occupies the whole length of the pipeline and P_u is the pressure in the upstream (closed) end of the pipeline, then the momentum equation is rearranged to find the pressure, P_u , at the sealed upstream end of the pipe:

$$P_u = P_{\text{sat}} + \frac{2fL_{\text{pipe}}G_{z1}^2}{D\rho_{\text{sat}}} \quad (32)$$

Using equation (27) the upstream density is therefore:

$$\rho_u = \rho_{\text{sat}} + \frac{\rho_0 - \rho_{\text{sat}}}{P_0 - P_{\text{sat}}} \frac{2fL_{\text{pipe}}G_{z1}^2}{D\rho_{\text{sat}}} \quad (33)$$

4.2.4 Mass in the Expanding Liquid Zone

The mass in zone 1 is calculated similarly to (29) from:

$$\frac{M_{z1}}{A_{\text{pipe}}} = \left[\rho_{\text{sat}}x + \frac{x^2 (\rho_u - \rho_{\text{sat}})}{2 L_{\text{pipe}}} \right]_0^{L_{\text{pipe}}} = L_{\text{pipe}} \frac{\rho_u + \rho_{\text{sat}}}{2} \quad (34)$$

where ρ_u is the density calculated at the upstream pressure P_u . The mass required to be lost to reach saturated conditions ($\Delta M_{L_{z1} > L_{\text{pipe}}}$) is therefore:

$$\Delta M_{L_{z1} > L_{\text{pipe}}} = M_0 - M_{\text{sat}} = A_{\text{pipe}} L_{\text{pipe}} \left(\rho_0 - \frac{\rho_u + \rho_{\text{sat}}}{2} \right) \quad (35)$$

Applying the relationship for the upstream density (31), the equation for $\Delta M_{L_{z1} > L_{\text{pipe}}}$ is $\Delta M_{L_{z1} > L_{\text{pipe}}}$ is:

$$\Delta M_{L_{z1} > L_{\text{pipe}}} = A_{\text{pipe}} L_{\text{pipe}} \left(\rho_0 - \rho_{\text{sat}} - \frac{\rho_0 - \rho_{\text{sat}}}{P_0 - P_{\text{sat}}} \frac{fL_{\text{pipe}}G_{z1}^2}{D\rho_{\text{sat}}} \right) \quad (36)$$

4.3 Discussion

This method described above is equivalent to the PiRRaM approach and has been included here for brevity. Equations (31) and (36) describe the amount of liquid necessary to be lost from the pipe for there to be a hypothetical expanding liquid zone, with a uniform pressure gradient along the pipe, dropping the pressure from the initial pressure to saturation. The two equations are necessary to describe the case where the expanding liquid zone exceeds the length of the pipe, and the case where the expanding liquid zone is less than the length of pipe. The latter case is novel in that, for a sufficiently long pipe, the initial mass flow rate decay is independent of the pipe length [see, (31)]. Moreover, the amount of mass required to be lost from the pipe to reach saturated conditions depends on the mass flow rate. Full-bore ruptures require only a small amount of mass to be removed from the pipe, whereas small holes need significantly more. The difference between equations (31) and (36) could be interpreted as when the liquid depressurisation can be treated as a pipe or a vessel respectively.

5 The Interpolation Method

To summarise, the initial mass flow rate ($\dot{m}_0 = A_{\text{hole}}G_0$) is calculated using the rarefaction balancing method described in Section 3. The mass flow rate at the beginning of saturated flow ($\dot{m}_{\text{sat}} = A_{\text{hole}}G_{\text{h,sat, choked}}$) is given by the PipeBreak choked saturated liquid mass flow rate calculation. The mass loss (ΔM) required to begin saturated flow is given by the equations (31) and (36) for the cases where the expanding zone is less ($\Delta M = \Delta M_{L_{\text{pipe}} > L_{12}}$), and greater ($\Delta M = \Delta M_{L_{z1} > L_{\text{pipe}}}$) than the pipe length respectively. To bridge the gap between the pressurised and saturated flow conditions interpolation is used.

PiRRaM assumes a method based upon the linear interpolation of \dot{m}^{-1} . The reasoning for this is that it is consistent with the underlying method used to propagate the solution, and the resulting interpolation places a lesser weighting on high mass flow rates. Arguably, there are infinitely many interpolations which are all equally valid. The PiRRaM approach is a pragmatic method which provides acceptable results, though for full bore ruptures and large holes it can predict that the elements of fluid have started to move at times earlier than a sound wave may have propagated there. This is not considered to be a significant deficiency, as it enables a smooth and consistent transition between the pressurised and saturated states across the range of modelled hole sizes. This approach also enables a complete solution to be derived, without the need for additional clarification or modelling decisions to be made (i.e. designed switches in model behaviour that often have unforeseen consequences).

Other interpolation methods were tested, but achieving a consistent well-behaved interpolation is nontrivial. PiRRaM uses the trapezoidal integration method to estimate the time step integral between conditions at step i and $i + 1$:

$$t_{i+1} - t_i = - \int_{M_i}^{M_{i+1}} \frac{1}{\dot{m}} dM = - \frac{1}{2} \left(\frac{1}{\dot{m}_{i+1}} + \frac{1}{\dot{m}_i} \right) (M_{i+1} - M_i) \quad (37)$$

This approach implicitly assumes a linear form for \dot{m}^{-1} over the interval of integration and is used as a motivation for a consistent interpolation function that enables the mass flow rate and pipe inventory to be calculated explicitly. The aim of this derivation is to find t , $M(t)$ and $\dot{m}(t)$ in the interval $[t_i, t_{i+1}]$, that are defined by $\dot{m}_i, M_i, \dot{m}_{i+1}$ and M_{i+1} (i.e. the quantities at each side of the interval) and that also satisfy:

$$\dot{m}(t) = - \frac{dM(t)}{dt} \quad (38)$$

For a scenario where $M_0, M_{\text{sat}}, \dot{m}_0, \dot{m}_{\text{sat}}$ and $t_0 = 0$ are known, t_{sat} is calculated from (37) as:

$$t_{\text{sat}} = \frac{1}{2} \left(\frac{1}{\dot{m}_0} + \frac{1}{\dot{m}_{\text{sat}}} \right) (M_0 - M_{\text{sat}}) \quad (39)$$

The interpolation function for the mass $M(t)$ and mass flow rate $\dot{m}(t)$ in the interval $[0, t_{\text{sat}}]$ are given by:

$$M(t) = \frac{-b \pm \sqrt{b^2 - 4ac(t)}}{2a} \quad \text{and} \quad \dot{m}(t) = [\dot{m}_0^{-1} + \psi(M(t) - M_0)]^{-1}, \quad (40)$$

where the variables a, b and $c(t)$ are found by evaluating the following expressions:

$$a = \frac{1}{2}\psi, \quad b = (\dot{m}_0^{-1} - \psi M_0) \quad c(t) = t - t_0 - aM_0^2 - bM_0, \quad \text{and} \quad \psi = \frac{\dot{m}_{\text{sat}}^{-1} - \dot{m}_0^{-1}}{M_{\text{sat}} - M_0} \quad (41)$$

This is valid provided that $\dot{m}_0 \neq \dot{m}_{\text{sat}}$. If $\dot{m}_0 = \dot{m}_{\text{sat}}$ then $\dot{m}(t) = \dot{m}_{\text{sat}}$ for t between 0 s and t_{sat} , which is generally expected for full-bore ruptures.

Ideally, an analytical solution could be used to fully characterise the transition between the frictionless pressurised liquid flow and the later friction dominated saturated flow. Unfortunately, an analytical solution to the early-stage evolution has not been forthcoming, and further work would be required to address this point. The approach adopted in PiRRaM is therefore a consistent and pragmatic solution which allows the solutions to transition between frictionless and friction flow in a simplified

manner. The approach has three features which make it well suited for its intended purpose. Firstly, for a sufficiently large pipe, the time corresponding to the start of saturated flow (t_{sat}) is independent of pipe length. Secondly, the loss mass required mass to reach saturated flow (ΔM) depends on the hole size, with smaller holes requiring more mass than large holes and full-bore ruptures. Thirdly, the model is robust and easily implemented without the need for complex numerical techniques. To summarise, the framework is applicable from full-bore rupture releases down to small hole releases, without the need to switch to either a vessel type model, or fundamentally change the structure of the model for small holes.

6 Model Sensitivity Testing

The initial release dynamics should be insensitive to the pipe length if it is sufficiently long. This is because a rarefaction wave must propagate the whole length of the pipe and back to affect the mass release rate. Figure 6 shows the PiRRaM prediction for the mass flow rate during the initial decompression of a full-bore rupture for the case of a 100 m (blue line), 200 m (orange line), 500 m (grey line) and 1000 km long pipeline (green dashed line). Also highlighted is the initial mass flow rate (\dot{m}_0), and mass flow rate at the beginning of the two-phase flow (\dot{m}_{sat}). The decompressions are characterised by an initially linear decay over the initial 200 ms to 400 ms due to the liquid expansion until saturated conditions are met (with the mass flow rate dropping from \dot{m}_0 to \dot{m}_{sat}), followed by a much steeper decay once the saturated two-phase flow ensues. The initial decay to saturated conditions is modelled using the interpolation method, followed by the two-phase model.

The length of the expanding liquid zone is approximately 270 m, in which case the initial decompression (between 0 and 400 ms with the mass flow rate dropping from \dot{m}_0 to \dot{m}_{sat}) becomes independent of the pipe length when the pipe length exceeds this value. Whilst pipe length affects the initial decompression for pipe lengths less than 270 m, this is acceptable given that the predictions are insensitive to pipe length for scenarios of more practical interest.

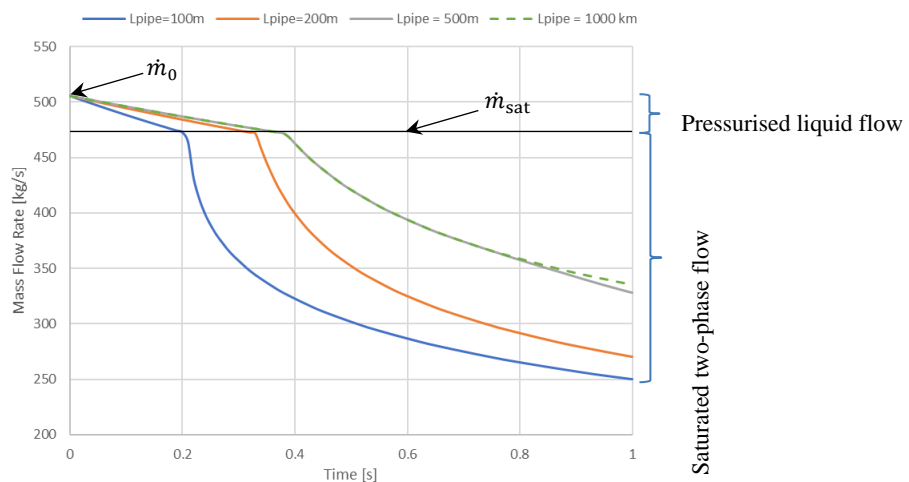


Figure 6 Plot showing the sensitivity of the initial duration of the transient decompression to pipe length. The interpolation is used to predict the mass flow rate variation between $\dot{m}_0 \approx 500$ kg/s and $\dot{m}_{\text{sat}} \approx 475$ kg/s.

7 Validation

7.1 Rarefaction Balancing Method

The rarefaction balancing method can be validated using CO2PipeTransData (Armstrong & Allason, 2014). Specifically, the pressure immediately upstream of the orifice plane can be used to examine the accuracy of the rarefaction balancing method. Table 1 shows a comparison of the pressures measured 25 cm upstream of the hole in the CO2PipeTrans experiments and the predictions of PiRRaM for the same location. PiRRaM matches the general trend and makes reasonable estimates of the measured values. Given that PiRRaM assumes isothermal decompression, an approximate linearised equation of state, and uses a very simple approach to quantify the complex release dynamics, the level of agreement is acceptable.

Table 1: Comparison of measured pressure 25 cm upstream of the hole and the prediction from PiRRaM

Trial	Relative hole size	Measured Pressure (bar)	PiRRaM Pressure (bar)
Test 6	4%	83.7	89.6
Test 5	16%	52.0	64.5
Test 7	28%	40.2	57.5
Test 3	45%	30.5	36.0
Test 4	100%	23.0	37.9

7.2 Interpolation method

Depending on the hole size, the flow in the earliest stages of these releases can be dominated by a rarefaction wave propagation. Capturing the time taken to reach saturated conditions whilst providing some insight into the likely transient behaviour during this period was a key requirement for PiRRaM.

The CO2PipeTrans experiments provide an excellent dataset to test the suitability of the interpolation method. Figure 7 shows comparisons between experimental data (black diamonds) and PiRRaM predictions (green lines) for the pressure¹⁰ immediately upstream of the orifice. For brevity, only phase 3 tests 4, 5, and 6, corresponding to FBR, 16% and 4% holes, are considered. The experimental data clearly shows a variety of different behaviours.

The plots show a steplike pressure decay for the smallest hole size (Figure 7, right), where the orifice pressure appears to jump between well-defined values before reaching the saturation pressure (≈ 32 bar) at 2.5 s after the pipe is opened. In contrast, in the full-bore rupture scenario (Figure 7, left) the decompression to saturated conditions (≈ 24 bar) near the opening plane is almost instantaneous. The middle hole size case (Figure 7, middle), shows only a single plateau in the pressure (≈ 46 bar) before reaching saturated conditions (≈ 32 bar at 0.9 s).

In the full-bore rupture case (Figure 7, left), saturated flow is predicted to be delayed by 0.05 s. In the 20% (Figure 7, middle) and 4% hole (Figure 7, right) scenarios, the predicted delay to saturated flow is 1.5 s and 6.4 s respectively. In each case the predicted time to reach saturated conditions is highlighted with the orange line. Whilst by no means perfect, PiRRaM can be seen to qualitatively capture the early transient decay of the pressure with an acceptable degree of accuracy. One of the requirements of the PiRRaM model is to accurately predict the decompression during the initial 30 s of the release.

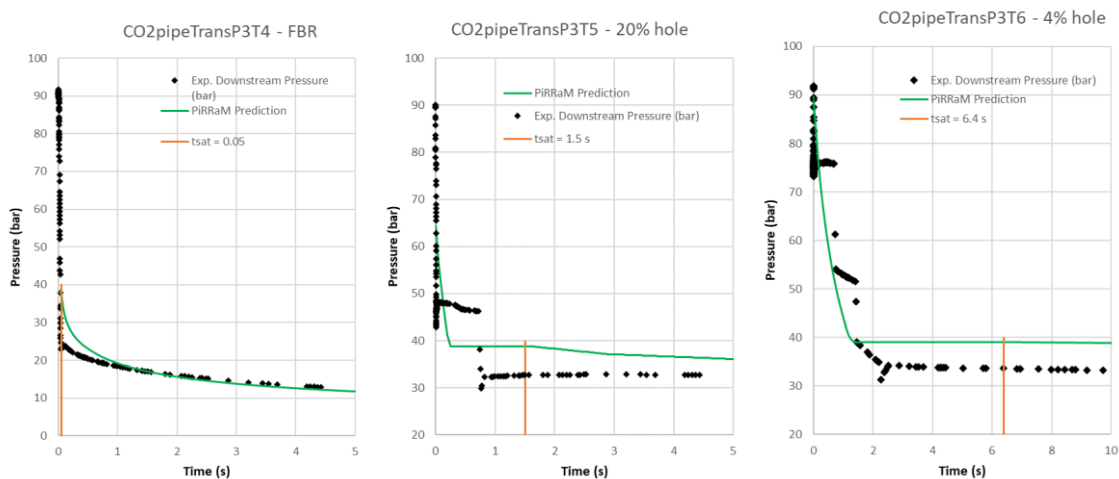


Figure 7 Comparison of the PiRRaM predictions (green lines) shown in comparison to the pressure decay measured immediately upstream of the orifice (black diamonds) for CO₂PipeTrans Phase 3 Test 4 (FBR, left plot), Test 5 (20% hole, middle plot), and Test 6 (4% hole, right plot). The orange line indicates the time at which the saturated solution begins.

¹⁰ For a given mass flow rate, the pressure is estimated finding P_d satisfying $A_{\text{hole}} C_d \sqrt{2\rho_{\text{liq}}(P_d - P_{\text{atm}})} = \dot{m}$. If P_d is estimated to be smaller than P_{sat} , then $P_d = P_{\text{sat}}$.

8 Summary

This paper describes a series of calculations which are used to estimate the mass flow rate during the initial decompression of a transportation pipeline containing a pressure liquified fluid. Whilst elements of the early decompression modelling in the PiRRaM method are pragmatic approaches, they provide a robust framework upon which to quantify the mass flow rate evolution.

There are various approaches which can be adopted to incorporate pressurised liquid effects into a saturated flow model, and several techniques were considered during the development of PiRRaM. One approach which appears to be particularly attractive, is to estimate the additional mass, due to the liquid pressurisation effect which is in excess to assuming saturated initial condition, and develop a technique through which this can be ejected before the saturated flow model is applied. However, this approach is problematic in that the initial release dynamics are then intrinsically coupled to the length of pipe. That is, as the length of pipe extends, the time taken to reach saturated conditions grows. In PiRRaM, the mass required to transition to the saturated flow solution depends on the hole size, with less mass required to transition for full-bore ruptures than for small holes. In this case, the sensitivity of the initial release dynamics to the pipe length disappears for sufficiently long pipes. Model sensitivity testing has been performed to demonstrate the insensitivity of the initial release dynamics to pipe length for practical scenarios.

The PiRRaM method has been compared to the initial stages of the CO2PipeTrans experiments. This included comparisons of the predicted pressure immediately upstream of the release to the experimentally measured values for different hole sizes, and comparison of the initial transient decompression. The comparison demonstrates that the rarefaction balancing technique captures the key dynamics occurring at the time of the ruptures, although the accuracy of predictions would likely be improved with better equation of state modelling. The interpolation method is shown to be suitable for its intended use in qualitatively capturing the key dynamics of characteristics of the initial pressure variation.

The method described in this paper considers releases from a single pipe. The solution can be easily adapted for symmetrical mid-point releases by modifying the rarefaction balancing equation to include an additional factor of two to account for the rarefaction wave propagating in opposite directions; choosing a pipe length to be half the actual pipe length; and doubling the mass flow rate in the full-bore rupture release case. A summary of the entire calculation, with notes to aid implementation, is given in the Appendix.

Authorship

The author confirms sole responsibility for the following: study conception and design; data collection; analysis and interpretation of results; and manuscript preparation.

Acknowledgements

The author gratefully acknowledges Zoe Chaplin, Liam Gray and Simon Coldrick from HSE, and Gemma Tickle of GT Science and Software, for their editorial and technical comments which have helped improve the manuscript.

Disclaimer

This publication and the work it describes was funded by the Health and Safety Executive (HSE). Its contents, including any opinions and/or conclusions expressed, are those of the authors alone and do not necessarily reflect HSE policy.

© Crown copyright (2024)

9 References

- Armstrong, K., & Allason, D. (2014). 2" NB shock-tube release of Dense Phase CO₂, GL-Noble Denton Technical report, . Phase 3 of the CO2PipeTrans project, available from DNV's website.
- Britter, R., Weil, J., Leung, J., & Hanna, S. (2011). Toxic industrial chemical (TIC) source emissions modeling for pressurized liquefied gases. *Atmospheric Environment*, 45(1), 1-25.
<https://doi.org/10.1016/j.atmosenv.2010.09.021>
- DNV. (2011). DISC Theory Document (Phast V6.7 Technical Documentation). DNV
- Haaland, S. E. (1983). Simple and explicit formulas for the friction factor in turbulent pipe flow.
- Landau, L. D., & Lifshitz, E. M. (1987). *Fluid mechanics: Landau And Lifshitz: course of theoretical physics, Volume 6* (Second Edition ed., Vol. 6). Pergamon Books Limited.
- Mahgerefteh, H., Jalali, N., & Fernandez, M. I. (2011). When does a vessel become a pipe?, *AIChE journal*, 57(12), 3305-3314.
- Newton, A. (2022). Pipeline Release Rate Model for pressure liquedified flows. *Hazards 32, Symposium Series*.
https://www.researchgate.net/publication/365623566_Pipeline_Release_Rate_Model_PiRRaM_for_Pressure_Liquedified_Gases

- Oke, A., Mahgerefteh, H., Economou, I., & Rykov, Y. (2003). A transient outflow model for pipeline puncture. *Chemical engineering science*, 58(20), 4591-4604.
- Reid, R. C., Poling, J. M., & Prausnitz, B. E. (1987). *The properties of gases and liquids* (4th Edition ed.). McGraw-Hill.
- Richardson, S., & Saville, G. (1996). Isle of Grain pipeline depressurisation tests. (OTH-94-441).
- Richardson, S., Saville, G., Fisher, S., Meredith, A., & Dix, M. (2006). Experimental determination of two-phase flow rates of hydrocarbons through restrictions. *Process Safety and Environmental Protection*, 84(1), 40-53.
- Webber, D., Fannelop, T., & Witlox, H. (1999, September). Source terms from two-phase flow in long pipelines following an accidental breach. *International Conference and Workshop on Modelling the Consequences of Accidental Releases of Hazardous Materials, CCPS, San Francisco, California*.
- Webber, D. M., Wardman, M., & Hirst, I. (2010). An investigation into the performance of the PipeTech Computer code in calculating the Isle of Grain pipeline blowdown tests. *HSE Research Report RR774*.
- Yi, J., & Mahgerefteh, H. (2020). An Analytically Based Pressurised Pipeline Decompression Model. *Hazards 30 Symposium Series*.

10 Appendix: Summary of Key Parameters and Equations

The table below provides a summary of the parameters and calculations necessary to evaluate the PiRRaM pressurised liquid decompression method.

Parameter	Notes
T_0, P_0	Initial temperature and pressure
$L_{\text{pipe}}, D_{\text{pipe}}, D_{\text{hole}}$ and ϵ	Pipe characteristics. For a midpoint release, L_{pipe} is chosen to be half the actual pipe length
P_{sat}	Saturated vapour pressure at initial temperature.
$\rho_0(T_0, P_0)$ and $\rho_{\text{sat}}(T_0, P_{\text{sat}})$	Initial and saturated liquid density . calculated using appropriate equation of state assuming isothermal liquid decompression
$M_0 = A_{\text{pipe}} \rho_0 L_{\text{pipe}}$	Initial mass in the pipe
$c_d = \begin{cases} 0.6 & \text{holes} \\ 1 & \text{FBR} \end{cases}$	Liquid coefficient of discharge.
$G_{\text{hole,liq,unchoked}} = c_d \sqrt{2\rho_{\text{sat}}(P_{\text{sat}} - P_{\text{atm}})}$	Saturated unchoked mass flux density
c_p	Liquid specific heat at constant pressure
$\phi(T_0) = T_0 \left. \frac{dP}{dT} \right _0$	Clausius Clapeyron relationship
$G_{\text{hole,sat,choked}} = \frac{\phi}{\sqrt{T_0 c_p - \phi \rho_{\text{sat}}^{-1}}}$	Choked liquid mass flux density
$c_{\text{sound}} = \sqrt{\frac{P_0 - P_d}{\rho_0 - \rho_d}}$	Liquid sound speed
$G_{\text{rarefaction}} = c_{\text{sound}}(\rho_0 - \rho_d)$	Rarefaction mass flux density
$\omega = \frac{c_{\text{sound}}}{P_{\text{sat}}} G_{\text{hole,liq,unchoked}}$	Criterion defining saturated pressurised liquid outflow
$\Omega = \frac{c_{\text{sound}}}{P_{\text{sat}}} G_{\text{hole,sat,choked}}$	Criterion defining saturated choked liquid outflow
$A_{\text{hole}}^* = A_{\text{hole}} A_{\text{pipe}}^{-1}$, and $P_0^* = P_0 P_{\text{sat}}^{-1}$	Dimensionless area and pressure
$m_0 = \begin{cases} A_{\text{hole}} G_{\text{hole,liq,unchoked}} & P_0^* \geq 1 + \omega A_{\text{hole}}^* \\ A_{\text{pipe}} G_{\text{rarefaction}} & 1 + \Omega A_{\text{hole}}^* \leq P_0^* < 1 + \omega A_{\text{hole}}^* \\ A_{\text{hole}} G_{\text{hole,sat,choked}} & P_0^* < 1 + \Omega A_{\text{hole}}^* \end{cases}$	Initial mass flow rate calculated using rarefaction balancing method. If a midpoint type release is considered, then A_{pipe} needs an additional factor of two to account for the rarefaction wave propagating in both directions for the hole case, or for a FBR, the midpoint release case.
$P_d = \begin{cases} P^* & G_{\text{rarefaction}} = A_{\text{hole}}^* G_{\text{hole,liq,unchoked}} & P_0^* \geq 1 + \omega A_{\text{hole}}^* \\ P_{\text{sat}} & 1 + \Omega A_{\text{hole}}^* \leq P_0^* < 1 + \omega A_{\text{hole}}^* \\ P_{\text{sat}} & P_0^* < 1 + \Omega A_{\text{hole}}^* \end{cases}$	Pressure downstream of rarefaction wave /immediately upstream of hole or pipe end. If a midpoint type release is considered, then A_{pipe} needs an additional factor of two to account for the rarefaction wave propagating in both directions from the hole.

Parameter	Notes
$\dot{m}_{\text{sat}} = A_{\text{hole}} \bar{G}_{\text{h,sat,choke}}$	Saturated mass flow mass flow rate. For a midpoint FBR type release, an additional factor of two will be required to account for contributions from both sides.
$L_{z1} = \frac{D_{\text{pipe}} \rho_{\text{sat}} (P_0 - P_{\text{sat}})}{2fG_{z1}^2}$	Length of the expanding liquid zone
$f = \left(4 \log_{10} \frac{3.7D_{\text{pipe}}}{\epsilon} \right)^{-2}$	Haaland correlation for calculating the Fanning friction factor
$\Delta M_{L_{\text{pipe}} > L_{z1z}} = A_{\text{pipe}} L_{z1} \left(\frac{\rho_0 - \rho_{\text{sat}}}{2} \right)$	Mass required to be lost to reach saturated conditions when $L_{\text{pipe}} > L_{z1}$
$\Delta M_{L_{z1} > L_{\text{pipe}}} = A_{\text{pipe}} L_{\text{pipe}} \left(\rho_0 - \rho_{\text{sat}} - \frac{\rho_0 - \rho_{\text{sat}}}{P_0 - P_{\text{sat}}} \frac{f L_{\text{pipe}} G_{z1}^2}{D \rho_{\text{sat}}} \right)$	Mass required to be lost to reach saturated conditions when $L_{\text{pipe}} < L_{z1}$.
$\Delta M = \begin{cases} \Delta M_{L_{\text{pipe}} > L_{z1}} & L_{\text{pipe}} > L_{z1} \\ \Delta M_{L_{z1} > L_{\text{pipe}}} & L_{\text{pipe}} < L_{z1} \end{cases}$	Evaluation of mass change
$t_{\text{sat}} = \frac{1}{2} \left(\frac{1}{\dot{m}_0} + \frac{1}{\dot{m}_{\text{sat}}} \right) \Delta M$	Time at which saturated solution begins
$a = \frac{1}{2} \psi, b = (\dot{m}_0^{-1} - \psi M_0), c(t) = t - t_0 - aM_0^2 - bM_0,$ and $\psi = \frac{\dot{m}_{\text{sat}}^{-1} - \dot{m}_0^{-1}}{-\Delta M}$	Constants for interpolation functions
$M(t) = \frac{-b \pm \sqrt{b^2 - 4ac(t)}}{2a}$ $\dot{m}(t) = \frac{1}{\dot{m}_0^{-1} + \psi(M(t) - M_0)}$	Interpolation functions for mass and mass flow rate for time between 0 s and t_{sat}